arXiv:1910.12880v1 [hep-ph] 28 Oct 2019

October 2019

A thermal neutrino interaction rate at NLO

G. Jackson and M. Laine

AEC, Institute for Theoretical Physics, University of Bern,
Sidlerstrasse 5, CH-3012 Bern, Switzerland

Abstract

The interaction rate of an ultrarelativistic active neutrino at a temperature below the electroweak crossover plays a role in leptogenesis scenarios based on oscillations between active neutrinos and GeV-scale sterile neutrinos. By making use of a Euclideanization property of a thermal light-cone correlator, we determine the $\mathcal{O}(g)$ correction to such an interaction rate in the high-temperature limit $\pi T \gg m_{_W}$, finding a $\sim 15...40\%$ reduction. For a benchmark point, this NLO correction decreases the lepton asymmetries produced by $\sim 1\%$.

1. Introduction

Completing the Standard Model with GeV-scale sterile neutrinos has become popular in recent years, given that they may account for the observed active neutrino mass differences and mixing angles through the seesaw mechanism [1–3], play a role in cosmology [4,5], and be searched for experimentally (for a review cf., e.g., ref. [6]). Apart from generating a baryon asymmetry (cf., e.g., refs. [7–12] and references therein), their dynamics could lead to the generation of lepton asymmetries larger than the baryon asymmetry [13–16], which could influence late-time cosmology, such as dark matter production [17–19].

If right-handed neutrinos are added to the Standard Model in a minimal renormalizable way, without introducing any other dynamical fields, then the neutrino sector is fully characterized by the values of Majorana mass parameters and neutrino Yukawa couplings. Even if this amounts to a large-dimensional parameter space, the values of the parameters start to be constrained. Therefore, it is important to scrutinize the precision of the theoretical computations on which the cosmological significance of this model relies. This is the goal of the present study. Specifically, we aim to determine one of the important rates, defined in eq. (2.1), up to next-to-leading order (NLO) in the weak-coupling expansion.

The computation of NLO corrections to real-time rates is a challenging task in the so-called ultrarelativistic regime $\pi T \gg m_i$, where m_i refers to the masses of the plasma particles, hampered as it is by powerlike infrared divergences which lead to the breakdown of the naive loop expansion.[1] In general, a nested resummation of the loop expansion is necessary for generating a consistent weak-coupling expansion. An important breakthrough was achieved in ref. [25], where it was realized that for many ultrarelativistic observables the real-time problem can be reduced to a static one. Then resummations can be implemented in a tractable fashion, which permitted for ref. [25] to recover previous results [26] in a simple way and to push the computation one order higher in the coupling. This insight has subsequently inspired, for instance, NLO determinations of the thermal photon [27] and soft dilepton [28] production rates from a QCD plasma; an estimate of the NLO contribution to its shear viscosity [29]; as well as attempts at incorporating the contribution of soft modes on a non-perturbative level, through numerical simulations of an effective theory [30–33].

The goal of the present paper is to adapt these techniques to the electroweak theory. Even though the SU(2) gauge coupling $g_2 \sim \frac{2}{3}$ is smaller than the QCD one, the NLO corrections are only suppressed by $g_2^2 T/(\pi m_i) \sim g_2/\pi$ (assuming $m_i \sim g_2 T$), and could come with large prefactors. Previously, they have been determined for so-called susceptibilities, relating chemical potentials to lepton asymmetries. As they were found to be numerically significant [34, 35], it appears well motivated to extend the exercise to a genuine rate observable.

[1] There are challenges also in the relativistic ($\pi T \sim m_i$) and non-relativistic ($\pi T \ll m_i$) regimes but those are of a different nature and parametrically less severe, cf. e.g. refs. [20–24].

2. Formulation of the problem

Denoting by $\mathcal{K} = (\omega, \mathbf{k})$ the four-momentum of an active neutrino propagating through a medium at a temperature T and by $\not{\Sigma}$ its (advanced) self-energy, the chiral nature of gauge interactions (cf. eq. (2.2)) implies that we may write [36]

$$\mathrm{Re}\,\not{\Sigma} \;=\; a\,\not{\mathcal{K}} + b\,\not{u}\;, \quad \mathrm{Im}\,\not{\Sigma} \;=\; \frac{1}{2}\Big(\Gamma_{\mathcal{K}}\,\not{\mathcal{K}} + \Gamma_u\,\not{u}\Big)\;, \tag{2.1}$$

where $u \equiv (1, \mathbf{0})$ denotes the four-velocity of the plasma in the local rest frame. The function a represents a radiative "wave function correction", whereas b can be interpreted as a thermal correction to a dispersion relation [36] (the full propagator is $\propto (\not{\mathcal{K}} + \not{\Sigma})^{-1}$). In the following, we are concerned with the interaction rate Γ_u. The rate $\Gamma_{\mathcal{K}}$ is relevant for the subleading helicity-flipping active-sterile transitions [37], however it was found in ref. [37], drawing upon earlier work in the QCD context [38, 39], that only the interaction rate Γ_u is susceptible to a simplified Euclideanized treatment *à la* ref. [25].

We assume that the neutrino is, to a good approximation, ultrarelativistic: $k \equiv |\mathbf{k}| \sim \pi T \gg M$, where $M = \sqrt{\omega^2 - k^2}$ denotes its virtuality. It interacts via weak interactions,

$$\mathcal{L}_M = \bar{\ell}_{\rm L} i\gamma^\mu D_\mu \ell_{\rm L}\;, \quad D_\mu = \partial_\mu - \frac{ig_1 B_\mu}{2} - \frac{ig_2\,\sigma^a A^a_\mu}{2}\;, \quad \ell_{\rm L} \;\equiv\; \begin{pmatrix} \nu_{\rm L} \\ e_{\rm L} \end{pmatrix}, \tag{2.2}$$

where g_1 is the hypercharge coupling, B_μ is the corresponding gauge potential, σ^a are the Pauli matrices, g_2 is the weak coupling and A^a_μ are the $\mathrm{SU_L}(2)$ gauge potentials.

In order to isolate the relevant helicity components, we employ the Weyl representation of the Dirac matrices: $\gamma^0\gamma^i = \mathrm{diag}(-\sigma^i, \sigma^i)$, $a_{\rm L} = \mathrm{diag}(\mathbb{1}, 0)$. Going to momentum space, $\partial_\mu \to i\mathcal{K}_\mu$, and aligning the momentum in the z-direction, the free part $\mathcal{L}_M \supset \nu^\dagger_{\rm L}(-\omega\mathbb{1} - k^z\sigma^z)\nu_{\rm L} + e^\dagger_{\rm L}(-\omega\mathbb{1} - k^z\sigma^z)e_{\rm L}$ implies that the lower (negative-helicity) components of $\nu_{\rm L}$ and $e_{\rm L}$ go on-shell for $\omega = k^z$. In the following we denote this component by ψ for $\nu_{\rm L}$, and by χ for $e_{\rm L}$. For these components, the coefficients of eq. (2.1) appear in the effective action as

$$\begin{aligned} \mathcal{S}_{M,\mathrm{eff}} \;\supset\; & \int_{\mathcal{K}} \psi^\dagger(\mathcal{K}) \left[\big(-\omega + k^z\big)\left(1 + a + \frac{i\Gamma_{\mathcal{K}}}{2}\right) - \left(b + \frac{i\Gamma_u}{2}\right)\right] \psi(\mathcal{K}) \\ + \;& \int_{\mathcal{K}} \chi^\dagger(\mathcal{K}) \left[\big(-\omega + k^z\big)\left(1 + \tilde{a} + \frac{i\tilde{\Gamma}_{\mathcal{K}}}{2}\right) - \left(\tilde{b} + \frac{i\tilde{\Gamma}_u}{2}\right)\right] \chi(\mathcal{K})\;, \end{aligned} \tag{2.3}$$

where $\tilde{a}, \tilde{b}, \tilde{\Gamma}_{\mathcal{K}}, \tilde{\Gamma}_u$ refer to the properties of left-handed electrons.

Following ref. [25], the idea now is to expand in fluctuations around the on-shell point, and then to rotate the light-like propagation into a static one. Simultaneously, we go over to Euclidean conventions, *viz.* $A^M_0 = iA^E_0$, and define a Euclidean Lagrangian as $L_E \equiv -\mathcal{L}_M$. Linear combinations of gauge potentials are denoted by $W^\pm_\mu \;\equiv\; (A^1_\mu \mp iA^2_\mu)/\sqrt{2}$, $\tilde{g}Z_\mu \;\equiv$

$g_1 B_\mu + g_2 A^3_\mu$, $\tilde{g} Z'_\mu \equiv g_1 B_\mu - g_2 A^3_\mu$, where $\tilde{g} \equiv \sqrt{g_1^2 + g_2^2}$. Then static fluctuations around the on-shell point are described by

$$L_E = -\begin{pmatrix} \psi \\ \chi \end{pmatrix}^\dagger \begin{Bmatrix} i\partial_z + \frac{\tilde{g}}{2}(iZ_0 + Z_3) & \frac{g_2}{\sqrt{2}}(iW_0^+ + W_3^+) \\ \frac{g_2}{\sqrt{2}}(iW_0^- + W_3^-) & i\partial_z + \frac{\tilde{g}}{2}(iZ'_0 + Z'_3) \end{Bmatrix} \begin{pmatrix} \psi \\ \chi \end{pmatrix} . \tag{2.4}$$

The "large" ω and k^z have cancelled against each other, so the "residual" momentum generated by $i\partial_z$ in eq. (2.4) can be taken to be small (it is denoted by k_z and is $\sim \tilde{g}^2 T$).

With the Lagrangian of eq. (2.4), we compute the Euclidean version of eq. (2.3). For nearly on-shell neutrinos, it takes the form[2]

$$S_{E,\mathrm{eff}} \supset \int_{\mathbf{k}} \psi^\dagger(\mathbf{k}) \left[k_z + \Sigma(k_z) \right] \psi(\mathbf{k}) \; , \quad \Sigma(k_z) = k_z \left(a + \frac{i\Gamma_{\mathcal{K}}}{2} \right) + b + \frac{i\Gamma_u}{2} + \mathcal{O}(k_z^2) \; . \tag{2.5}$$

It turns out that within the effective theory, the real part of Σ is odd in k_z and the imaginary part is even in k_z, guaranteeing that correlations decay exponentially (i.e. that the pole is on the imaginary axis). Consequently, only a and Γ_u are generated within our computation, as already alluded to above.

It can be deduced from eq. (2.5) that the free neutrino and electron propagators have the forms

$$\langle \psi(\mathbf{k}) \psi^\dagger(\mathbf{q}) \rangle_0 = \frac{(2\pi)^d \delta^{(d)}(\mathbf{k} - \mathbf{q})}{k_z + i0^+} = \langle \chi(\mathbf{k}) \chi^\dagger(\mathbf{q}) \rangle_0 \; , \tag{2.6}$$

where $d = 3 - 2\epsilon$. The other propagators are those of the dimensionally reduced theory for the Standard Model [40], with the temporal gauge field components A_0^a and B_0 kept as dynamical fields. We carry out computations in a general R_ξ gauge, whereby the spatial $W^\pm$ propagator reads ($a', b' \in \{1, 2\}$)

$$\left\langle A_i^{a'}(\mathbf{k}) A_j^{b'}(\mathbf{q}) \right\rangle_0 = \delta^{a'b'} T (2\pi)^d \delta^{(d)}(\mathbf{k} + \mathbf{q}) \left\{ \frac{\delta_{ij}}{k^2 + m_W^2} + \frac{k_i k_j}{m_W^2} \left(\frac{1}{k^2 + m_W^2} - \frac{1}{k^2 + \xi m_W^2} \right) \right\} . \tag{2.7}$$

There are similar propagators for the neutral components Z_i and Q_i which, as usual, are obtained from A_i^3 and B_i by a rotation with the mixing angle $\sin(2\theta) = 2g_1 g_2/(g_1^2 + g_2^2)$.

For the temporal components Z_0 and Q_0, the mixing is modified by thermal (Debye) masses. Let us denote the mixing angle of the temporal components by $\tilde{\theta}$. Following ref. [41], the masses of the diagonalized modes are denoted by $m_{\widetilde{Z}}^2$ and $m_{\widetilde{Q}}^2$. The original gauge fields can be expressed in the new basis as

$$Z_0 = \cos(\theta - \tilde{\theta})\, \widetilde{Z}_0 + \sin(\theta - \tilde{\theta})\, \widetilde{Q}_0 \; , \quad Z'_0 = -\cos(\theta + \tilde{\theta})\, \widetilde{Z}_0 + \sin(\theta + \tilde{\theta})\, \widetilde{Q}_0 \; , \tag{2.8}$$

[2]The original ψ has been scaled by a factor $T^{1/2}$ so that $\psi(\mathbf{x})$ has the dimension GeV and $\psi(\mathbf{k})$ the dimension GeV^{-2}. The same dimensions apply to the gauge potentials $A_\mu^a(\mathbf{x})$ and $A_\mu^a(\mathbf{k})$, respectively.



Figure 1: Leading-order contributions to self-energy. A double line denotes a neutrino (ψ) propagator from eq. (2.6); a filled blob an electron (χ) propagator; a wiggly line a spatial gauge field; and a solid line a temporal gauge field, which in the effective theory has turned into an adjoint scalar field.

and the corresponding propagators take the forms

$$\left\langle W_0^+(\mathbf{k})W_0^-(\mathbf{q})\right\rangle_0 \;=\; T(2\pi)^d\delta^{(d)}(\mathbf{k}+\mathbf{q})\,\frac{1}{k^2+m_{\widetilde{W}}^2}\;, \tag{2.9}$$

$$\left\langle Z_0(\mathbf{k})Z_0(\mathbf{q})\right\rangle_0 \;=\; T(2\pi)^d\delta^{(d)}(\mathbf{k}+\mathbf{q})\left[\frac{\cos^2(\theta-\tilde{\theta})}{k^2+m_{\widetilde{Z}}^2}+\frac{\sin^2(\theta-\tilde{\theta})}{k^2+m_{\widetilde{Q}}^2}\right], \tag{2.10}$$

$$\left\langle Z_0'(\mathbf{k})Z_0'(\mathbf{q})\right\rangle_0 \;=\; T(2\pi)^d\delta^{(d)}(\mathbf{k}+\mathbf{q})\left[\frac{\cos^2(\theta+\tilde{\theta})}{k^2+m_{\widetilde{Z}}^2}+\frac{\sin^2(\theta+\tilde{\theta})}{k^2+m_{\widetilde{Q}}^2}\right]. \tag{2.11}$$

The relations between $m_{\widetilde{W}}^2$, $m_{\widetilde{Z}}^2$, $m_{\widetilde{Q}}^2$ and the angles $\theta,\tilde{\theta}$ satisfy identities which are not always easy to recognize at first sight, e.g.

$$m_{\widetilde{Z}}^2-m_{\widetilde{W}}^2 \;=\; m_W^2\tan(\theta)\tan(\tilde{\theta})\;,\quad m_{\widetilde{W}}^2-m_{\widetilde{Q}}^2 \;=\; m_W^2\tan(\theta)\cot(\tilde{\theta})\;. \tag{2.12}$$

Let us end this section by commenting upon differences with respect to the observable analyzed in the QCD context [25]. The quantity considered there was a Wilson loop rather than a single propagator (which can be interpreted as a Wilson line). The transverse coordinate of the loop, $r_\perp$, served to define a "collision kernel", $C(q_\perp)$, and the so-called jet quenching parameter, $\hat{q}$, is a weighted integral over $C(q_\perp)$. The weighting by $q_\perp^2$ implies that the soft contribution to $\hat{q}$ is UV divergent. In our case there is no such weighting, and Γ_u is UV finite. On the other hand, the absence of weighting makes Γ_u more IR sensitive than $\hat{q}$, and therefore Γ_u is perturbatively computable only in the Higgs phase.

3. Leading-order computation

The leading contribution to Γ_u originates at 1-loop level, through the graphs shown in fig. 1.

Inserting the propagators from eqs. (2.6), (2.7), (2.9) and (2.10) and denoting the internal momentum by $\mathbf{p}=\mathbf{p}_\perp+p_z\mathbf{e}_z$, we are faced with integrals of the type

$$I(k_z)=T\int_{\mathbf{p}}\frac{1}{k_z-p_z+i0^+}\frac{1}{p_z^2+\epsilon_p^2}\;,\quad \epsilon_p^2\;\equiv\;p_\perp^2+m^2\;. \tag{3.1}$$

Noting that the external momentum $k_z \sim \tilde{g}^2 T$ is small compared with the mass scales $m_i \sim \tilde{g}T$, we can expand in k_z. Evaluating the integral over p_z with the residue theorem, or with

$$\frac{1}{p_z - k_z - i0^+} = \mathbb{P}\biggl(\frac{1}{p_z - k_z}\biggr) + i\pi\delta(p_z - k_z)\,, \tag{3.2}$$

where $\mathbb{P}$ denotes a principal value, yields

$$I(k_z) \approx T\biggl\{\frac{i}{2}\int_{\mathbf{p}_\perp}\frac{1}{\epsilon_p^2} + k_z\int_{\mathbf{p}}\mathbb{P}\biggl[\frac{1}{p_z^2(p_z^2+\epsilon_p^2)}\biggr] + \mathcal{O}(k_z^2)\biggr\}\,. \tag{3.3}$$

The first term contributes directly to the width, whereas the second one gives a wave function correction, proportional to k_z (cf. eq. (2.5)). The wave function corrections are gauge dependent and IR-sensitive, but they do play a role in cancelling similar effects from loop diagrams. Therefore they need to be accounted for at NLO, as discussed in appendix A.7.

Focussing now on the leading-order (LO) width, which originates from the first term in eq. (3.3), it is straightforward to verify that there is no gauge parameter dependence. Summing together the graphs, we obtain ($\Delta_i \equiv (p_\perp^2 + m_i^2)^{-1}$)

$$\Gamma_u^{(\mathrm{LO})} = \frac{\tilde{g}^2 T}{4}\int_{\mathbf{p}_\perp}\Bigl\{\Delta_{Z} - \cos^2(\theta-\tilde{\theta})\Delta_{\tilde{Z}} - \sin^2(\theta-\tilde{\theta})\Delta_{\tilde{Q}} + 2\cos^2(\theta)\bigl(\Delta_{W} - \Delta_{\widetilde{W}}\bigr)\Bigr\}\,. \tag{3.4}$$

It remains to carry out the integral over the transverse momentum $\mathbf{p}_\perp$. Even if the whole integral is UV finite, it was argued in ref. [37] that it is reasonable to adopt a phenomenological cutoff $|\mathbf{p}_\perp| \leq 2k \sim 2\pi T$. Adopting this prescription, which amounts to a partial inclusion of higher order contributions in an expansion in $\sim m_i^2/k^2$, transverse integrals evaluate to

$$\int_{|\mathbf{p}_\perp|\leq 2k}\frac{1}{p_\perp^2 + m^2} \;=\; \frac{\ln\bigl(1+4k^2/m^2\bigr)}{4\pi}\,. \tag{3.5}$$

Thereby eq. (3.4) reproduces the LO result for Γ_u as given in eq. (5.23) of ref. [37].

4. NLO result and some of its features

Proceeding to the NLO level, there are a number of contributions, listed in appendix A. Summing them together, the result can be expressed as

$$\Gamma_u^{(\mathrm{NLO})} \;=\; \frac{\tilde{g}^4 T^2}{8}\lim_{m_Q\to 0}\int_{\mathbf{p}_\perp}\biggl\{\sum_i\bigl(\,c_i A_i + \dot{c}_i\dot{A}_i\,\bigr) + \sum_{i,j}\bigl(\,c_{ij}B_{ij} + c_{ij}^T B_{T,ij} + \dot{c}_{ij}\dot{B}_{ij}\,\bigr)\biggr\}\,, \tag{4.1}$$

where $c_i, \dot{c}_i, c_{ij}, c_{ij}^T, \dot{c}_{ij}$ are coefficients and $i,j = \{H, Z, \ldots\}$ label particles appearing in the loops. The "photon mass" m_Q was introduced as an intermediate IR regulator (see below).

Making use of the notation of appendix A.1, simplified further by denoting $A_i \equiv A(m_i)$, etc, the linear combinations needed in eq. (4.1) read[3]

$$
\begin{aligned}
\sum_i c_i A_i \;=\; & \qquad (4.2)\\
& \Big\{A_H + \frac{m_Z^2}{m_H^2}\big[(d-1)A_Z + \cos^2(\theta-\tilde\theta)A_{\tilde Z} + \sin^2(\theta-\tilde\theta)A_{\tilde Q}\big] + \frac{2m_W^2}{m_H^2}\big[\,(d-1)A_W + A_{\widetilde W}\,\big]\Big\}\\
& \times\Big\{\;\Delta_Z^2 - \big[\cos^2(\theta-\tilde\theta)\Delta_{\tilde Z} + \sin^2(\theta-\tilde\theta)\Delta_{\tilde Q}\big]^2 + 2\cos^4(\theta)\big(\Delta_W^2 - \Delta_{\widetilde W}^2\big)\;\Big\}\\
-\;& 4\cos^4(\theta)\,\big[(d-2)\cos^2(\theta)A_Z + \cos^2(\tilde\theta)A_{\tilde Z} + \sin^2(\tilde\theta)A_{\tilde Q} + (d-2)A_W + A_{\widetilde W}\big]\big(\Delta_W^2 - \Delta_{\widetilde W}^2\big)\\
+\;& 4\cos^2(\theta)\,\big[(d-2)A_W + A_{\widetilde W}\big]\\
& \times\big\{\big[\cos(\tilde\theta)\cos(\theta-\tilde\theta)\Delta_{\tilde Z} - \sin(\tilde\theta)\sin(\theta-\tilde\theta)\Delta_{\tilde Q}\big]^2 - \cos^2(\theta)\,\Delta_Z^2\big\}\\
+\;& A_W\sin(2\theta)\,\big\{\sin(2\theta)\Delta_Z^2 + \sin(2\tilde\theta)\big[\sin^2(\theta-\tilde\theta)\Delta_{\tilde Q}^2 - \cos^2(\theta-\tilde\theta)\Delta_{\tilde Z}^2\big]\\
& -\cos(2\tilde\theta)\sin[2(\theta-\tilde\theta)]\Delta_{\tilde Q}\Delta_{\tilde Z}\big\}\;,
\end{aligned}
$$

$$
\begin{aligned}
\sum_i \dot c_i \dot A_i \;=\; & \qquad (4.3)\\
& 8\cos^4(\theta)\,\big[\cos^2(\theta)\dot A_Z - \cos^2(\tilde\theta)\dot A_{\tilde Z} + \sin^2(\theta)\dot A_Q - \sin^2(\tilde\theta)\dot A_{\tilde Q} + \dot A_W - \dot A_{\widetilde W}\big]\big(\Delta_{\widetilde W} - \Delta_W\big)\\
+\;& 8\cos^3(\theta)\,\big(\,\dot A_W - \dot A_{\widetilde W}\,\big)\big[\,\cos(\tilde\theta)\cos(\theta-\tilde\theta)\Delta_{\tilde Z} - \sin(\tilde\theta)\sin(\theta-\tilde\theta)\Delta_{\tilde Q} - \cos(\theta)\Delta_Z\,\big]\;,
\end{aligned}
$$

$$
\begin{aligned}
\sum_{i,j} c_{ij} B_{ij} \;=\; & \qquad (4.4)\\
& 2m_Z^2\,B_{HZ}\,\Delta_Z^2\\
-\;& 2m_Z^2\big[\cos^2(\theta-\tilde\theta)B_{H\tilde Z} + \sin^2(\theta-\tilde\theta)B_{H\tilde Q}\big]\big[\cos^2(\theta-\tilde\theta)\Delta_{\tilde Z} + \sin^2(\theta-\tilde\theta)\Delta_{\tilde Q}\big]^2\\
+\;& 4m_W^2\cos^4(\theta)\big[\;\big(B_{HW} + B_{ZW}\big)\,\Delta_W^2 - \big(B_{H\widetilde W} + B_{Z\widetilde W}\big)\,\Delta_{\widetilde W}^2\;\big]\\
-\;& 4m_W^2\cos^2(\theta)\,\big[\cos^2(\theta+\tilde\theta)B_{\tilde Z W} + \sin^2(\theta+\tilde\theta)B_{\tilde Q W}\big]\,\Delta_{\widetilde W}^2\\
+\;& 16\cos^4(\theta)\Big\{\;p_\perp^2\,\Big[\;\cos^2(\theta)\,\big(B_{ZW}\Delta_W^2 - B_{Z\widetilde W}\Delta_{\widetilde W}^2\big) + \;\sin^2(\theta)\,\big(B_{QW}\Delta_W^2 - B_{Q\widetilde W}\Delta_{\widetilde W}^2\big)\\
& -\big[\cos^2(\tilde\theta)B_{\tilde Z W} + \sin^2(\tilde\theta)B_{\tilde Q W}\big]\,\Delta_{\widetilde W}^2\Big] + \;\big[\cos^2(\tilde\theta)B_{\tilde Z\widetilde W} + \sin^2(\tilde\theta)B_{\tilde Q\widetilde W}\big]\,\Delta_W\;\Big\}\\
-\;& 4m_W^2(4\cos^2\theta - 1)\big[B_{WW}\Delta_Z^2 + \cos^2(\theta)\,B_{ZW}\,\Delta_W^2\big] + 8\cos^4(\theta)\,\big(B_{WW} + B_{\widetilde W\widetilde W}\big)\Delta_Z\\
+\;& \frac{4B_{W\widetilde W}}{m_Z^2}\,\Big\{\;\cos^2(\theta) - 2m_W^2\big[\cos^2(\theta-\tilde\theta)\,\Delta_{\tilde Z} + \sin^2(\theta-\tilde\theta)\,\Delta_{\tilde Q}\big]\\
& -\big[(m_W^2 - m_{\widetilde W}^2)^2 + 2p_\perp^2(m_W^2 + m_{\widetilde W}^2) + p_\perp^4\big]\\
& \times\big[\cos(\theta-\tilde\theta)\cos(\tilde\theta)\,\Delta_{\tilde Z} - \sin(\theta-\tilde\theta)\sin(\tilde\theta)\,\Delta_{\tilde Q}\big]^2\;\Big\}\;,
\end{aligned}
$$

$$
\sum_{i,j} c_{ij}^T B_{T,ij} \;= \qquad (4.5)
$$

[3]For convenience a *c*-program evaluating this expression is included as an ancillary file in the arXiv record.

$$
\begin{aligned}
& 2\big\{ B_{T,HZ} + \big[4(d-2)\cos^4(\theta) + \cos^2(2\theta)\big] B_{T,WW} + 4\cos^4(\theta)\, B_{T,\widetilde{W}\widetilde{W}} \big\}\, \Delta_Z^2 \\
+ \quad & 4\cos^4(\theta) \big\{ B_{T,HW} + \big[4(d-2)\cos^2\theta + 1\big] B_{T,ZW} + 4\cos^2(\tilde{\theta})\, B_{T,\tilde{Z}\widetilde{W}} \\
& + 4(d-2)\sin^2(\theta)\, B_{T,QW} + 4\sin^2(\tilde{\theta})\, B_{T,\tilde{Q}\widetilde{W}} \big\}\, \Delta_W^2 \;,
\end{aligned}
$$

$$
\begin{aligned}
& \sum_{i,j} \dot{c}_{ij} \dot{B}_{ij} \;= \qquad\qquad (4.6) \\
& 8\cos^4(\theta) \big\{ \;\cos^2(\theta) \big(\dot{B}_{ZW} - \dot{B}_{Z\widetilde{W}}\big) + \cos^2(\tilde{\theta}) \big(\dot{B}_{\tilde{Z}\widetilde{W}} - \dot{B}_{\tilde{Z}W}\big) \\
+ \quad & \sin^2(\theta) \big(\dot{B}_{QW} - \dot{B}_{Q\widetilde{W}}\big) + \sin^2(\tilde{\theta}) \big(\dot{B}_{\tilde{Q}\widetilde{W}} - \dot{B}_{\tilde{Q}W}\big) + \tfrac{1}{2} \big(\dot{B}_{WW} + \dot{B}_{\widetilde{W}\widetilde{W}}\big) - \dot{B}_{\widetilde{W}W} \;\big\} \;.
\end{aligned}
$$

The final integral over $\mathbf{p}_\perp$ is best performed numerically, within the domain of eq. (3.5).

Our result for $\Gamma_u^{(\mathrm{NLO})}$ passes a number of crosschecks. A simple one is that all gauge dependent pieces have cancelled. A less trivial test can be obtained by looking at the value of the integrand at $p_\perp^2 \gg m_i^2$. The leading term of the Taylor expansion, obtained by inserting eq. (A.6) as well as the asymptotics from eqs. (A.7) and (A.8), comes from the part $\sum_{i,j} c_{ij}^T B_{T,ij}$ in eq. (4.5). Here the different pieces add up, whereas all other structures contain a cancellation between spatial and temporal contributions. This yields

$$
\begin{aligned}
\Gamma_u^{(\mathrm{NLO})} \quad & \supset \quad \frac{\tilde{g}^4 T^2}{8} \int_{|\mathbf{p}_\perp| \gg m_i} \frac{4[3(2d-1)\cos^4(\theta) + \sin^4(\theta)] B_{T,00}}{p_\perp^4} \\
& \stackrel{d=3}{=} \; -\frac{\tilde{g}^4 T^2}{8} \int_{|\mathbf{p}_\perp| \gg m_i} \frac{15\cos^4(\theta) + \sin^4(\theta)}{16 p_\perp^3} \;, \qquad (4.7)
\end{aligned}
$$

where on the first line $B_{T,00}$ indicates that masses can be put to zero. This agrees perfectly with the NLO part of eq. (D.6) of ref. [41], which was obtained by considering the IR asymptotics of a fully relativistic but unresummed computation.

It is also good to check that the resummed expression is IR finite. As charged particles appear in the loops, massless photons do affect the NLO result. Some of their contributions are unproblematic, but there are certain terms where it needs to be verified that the limit $m_Q \to 0$ can indeed be taken in eq. (4.1). For this we note that

$$
\lim_{m_Q \to 0} \left[\dot{B}(m_Q, m) - \frac{\dot{A}(m_Q)}{p^2 + m^2} \right] \stackrel{d=3}{=} \frac{m^2 - p^2}{8\pi m (p^2 + m^2)^2} \;. \qquad (4.8)
$$

Indeed all m_Q-dependence of eqs. (4.3) and (4.6) appears in this IR-safe combination.

We plot the result from eq. (4.1), both as an integrand and after the integration, in fig. 2. For this, the parameters have been fixed as in ref. [37]. A partial cancellation between contributions from various domains of $p_\perp$ can be observed, as a result of which the final magnitude of the negative NLO correction remains at a modest $\sim 15\%$ level at high temperatures. It reaches $\sim 40\%$ at low temperatures, mostly because the LO contribution is "anomalously small" there due to a cancellation between the spatial and temporal contributions in eq. (3.4), *viz.* $\Gamma_u^{(\mathrm{LO})} \sim \tilde{g}^4 T^3 / m_i^2$ at $\tilde{g}T \ll m_i$, however in that region the approximation $m_i \ll \pi T$ inherent to our effective theory approach gradually breaks down.

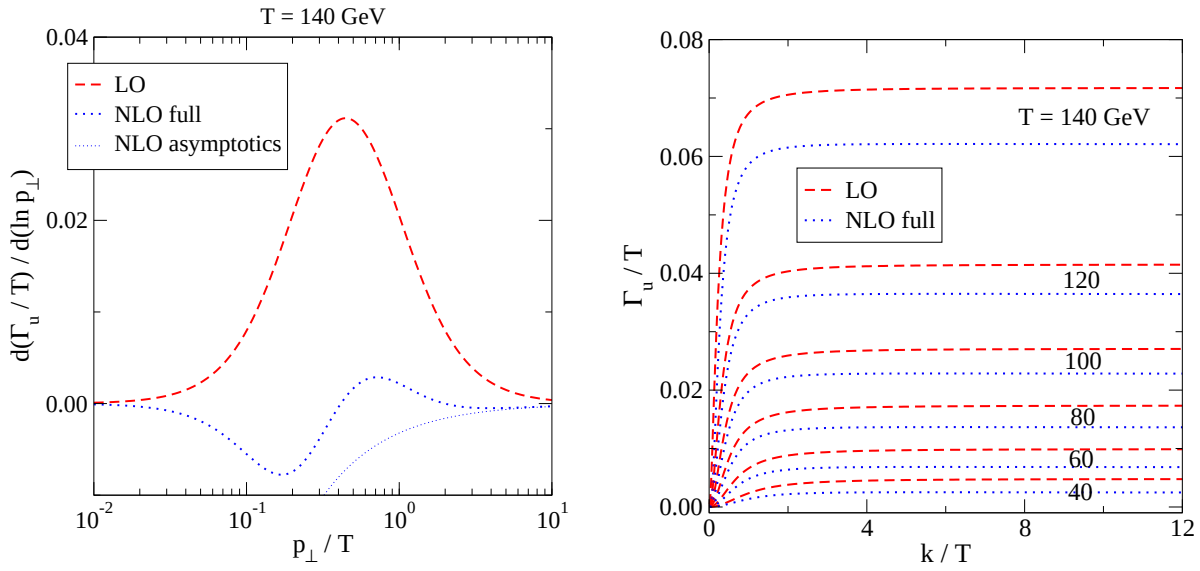


Figure 2: Left: the integrands from eqs. (3.4) (LO), (4.1) (NLO full) and (4.7) (NLO asymptotics), at $T \approx 140$ GeV. Right: the corresponding integrals, as a function of T and k (the latter originates as discussed around eq. (3.5)). At high T the NLO correction is seen to reduce the LO rate by $\sim 15\%$, at low T by $\sim 40\%$.

5. Summary and outlook

We have reported a thermal NLO computation of a neutrino interaction rate Γ_u, defined through eq. (2.1), in the temperature range $\pi T \gg m_W$. The final result is given in eq. (4.1) and plotted numerically in fig. 2, whereas many technical details are relegated into appendix A. The result passes a number of crosschecks, in particular it is gauge independent and displays the UV asymptotics predicted by an earlier unresummed computation. By taking $g_1 \to 0$, it can partially also be contrasted with the QCD result of ref. [25], even if the presence of a Higgs field and Higgs expectation value prohibit an unambiguous comparison.

The coefficient Γ_u is but one of a set of mass corrections and interaction rates entering a complete GeV-scale leptogenesis framework [37].[4] It is, however, the *first* ultrarelativistic rate that has been computed up to NLO for thermal neutrino physics. Even though it will take time before all other coefficients are known at the same level, we hope that the knowledge of one of them helps to motivate such efforts.

[4]More precisely, Γ_u determines the rate of helicity-conserving active-sterile oscillations, as

$$\Gamma \simeq \frac{h_\nu^2 v^2 M^2 \Gamma_u}{2[(M^2+2\omega b)^2 + (\omega\Gamma_u)^2]} \,, \tag{5.1}$$

where h_ν is a neutrino Yukawa coupling, v is the Higgs expectation value, $\omega \equiv \sqrt{k^2+M^2}$, M is the mass of a right-handed neutrino, and b is the correction parametrizing the real part of eq. (2.1).

A leptogenesis computation typically comes with two goals: determining the baryon asymmetry, which is fixed at $T \sim 130$ GeV when sphaleron processes switch off [42], and determining lepton asymmetries, which continue to be produced when $T < 130$ GeV. As the rate that we computed only concerns processes that are active in the Higgs phase (cf. eq. (5.1)), it is no surprise that it has little effect on the baryon asymmetry: we only observe a variation on the per mille level. The influence on lepton asymmetries is a bit larger, however by considering the benchmark point ■ from ref. [37], chosen because lepton asymmetry production continues for a long time in this case, we found a reduction of lepton asymmetries by $\sim 1\%$. Hence it appears that for practical applications it is sufficient to use the simple leading-order expression for Γ_u from eq. (3.4).

Closing on a conceptual note, our computation can be interpreted as amounting to determining the exponential fall-off of a single light-like Wilson line. Even though we have verified the independence of the result on the gauge fixing parameter up to NLO, the observable itself is not manifestly gauge invariant. Another possible starting point would be to consider a Wilson loop (like in ref. [32] but in the Higgs phase), which is gauge invariant. In this setup, the information relevant for us could be extracted by pulling the sides of the Wilson loop far from each other ($r_\perp \to \infty$), and interpreting the coefficient of the resulting decay as *twice* the width $\Gamma_u/2$ that we are interested in. Our approach has the technical advantage that it could be generalized, graph-by-graph, to determining the complete NLO self-energy of an active neutrino beyond the ultrarelativistic regime, even if the practical implementation of this generalization is challenging, given that a full 4d computation is required.

Acknowledgements

This work was partly supported by the Swiss National Science Foundation (SNF) under grant 200020B-188712.

Appendix A. Contributions from NLO diagrams

In this appendix we record the separate contributions to the function $\Sigma(k_z)$, defined in eq. (2.5). For momentum dependence, specifically $\Sigma'(0)$, it is sufficient to remain at 1-loop ("LO") level (cf. sec. A.7), whereas $\Sigma(0)$ is needed up to 2-loop level ("NLO"). For completeness we list results for a general R_ξ gauge. The gauge parameter appears in the masses of the longitudinal gauge bosons and Goldstone modes, which are denoted by

$$m'^2 \equiv \xi\, m^2 \,. \tag{A.1}$$

In terms which are not manifestly IR finite, we denote by m_Q a fictitious photon mass, which is taken to zero at the end of the computation.

A.1. Master functions

Denoting $q = (\mathbf{q}_\perp, q_z)$, $d \equiv 3-2\epsilon$, $\int_{\mathbf{q}} \equiv \int \frac{\mathrm{d}^d\mathbf{q}}{(2\pi)^d}$, and $\int_{\mathbf{q}_\perp} \equiv \int \frac{\mathrm{d}^{d-1}\mathbf{q}_\perp}{(2\pi)^{d-1}}$, the NLO result can be expressed in terms of the two master integrals

$$A(m) \equiv \int_{\mathbf{q}} \frac{1}{q^2+m^2} = \int_{\mathbf{q}_\perp} \frac{1}{2\epsilon_q} \stackrel{d=3}{=} -\frac{m}{4\pi}\,, \tag{A.2}$$

$$\begin{aligned} B(m_1,m_2) &\equiv \int_{\mathbf{q}} \frac{1}{(q^2+m_1^2)[(p+q)^2+m_2^2]} \stackrel{p_z=0}{=} \int_{\mathbf{q}_\perp} \frac{1}{2\epsilon_{q1}\epsilon_{pq2}(\epsilon_{q1}+\epsilon_{pq2})} \\ &\stackrel{d=3}{=} \frac{i}{8\pi p_\perp} \ln\frac{m_1+m_2-ip_\perp}{m_1+m_2+ip_\perp} = \frac{1}{4\pi p_\perp}\arctan\Big(\frac{p_\perp}{m_1+m_2}\Big)\,, \end{aligned} \tag{A.3}$$

where $\epsilon_{q1}^2 \equiv q_\perp^2 + m_1^2$ and $\epsilon_{pq2}^2 \equiv (p_\perp+q_\perp)^2 + m_2^2$. Sometimes we need the mass derivatives of these functions, defined as

$$\dot{A}(m) \equiv \frac{\mathrm{d}A(m)}{\mathrm{d}m^2}\,, \quad \dot{B}(m_1,m_2) \equiv \left(\frac{\partial}{\partial m_1^2} + \frac{\partial}{\partial m_2^2}\right) B(m_1,m_2)\,. \tag{A.4}$$

In addition it is convenient to define the tensor integral

$$B_{ij} \equiv \int_{\mathbf{q}} \frac{q_i q_j}{(q^2+m_1^2)[(p+q)^2+m_2^2]} \equiv \left(\delta_{ij} - \frac{p_i p_j}{p^2}\right) B_{_T} + \frac{p_i p_j}{p^2} B_{_L}\,. \tag{A.5}$$

In practice we need B_{zz} at $p_z = 0$, which is then given by $B_{zz}|_{p_z=0} = B_{_T}$. It is possible to express $B_{_T}$ in terms of the integrals in eqs. (A.2) and (A.3), as

$$\begin{aligned} B_{_T}(m_1,m_2) &= \frac{1}{4(d-1)p_\perp^2}\Big\{\big[p_\perp^2 - m_1^2 + m_2^2\big]\,A(m_1) + \big[p_\perp^2 + m_1^2 - m_2^2\big]\,A(m_2) \\ &\quad - \big[p_\perp^4 + 2p_\perp^2(m_1^2+m_2^2) + (m_1^2-m_2^2)^2\big]\,B(m_1,m_2)\Big\}\,, \end{aligned} \tag{A.6}$$

however it is more compact to display results in terms of $B_{_T}$, thereby avoiding inverse powers of $p_\perp^2$ and $d-1$. We note that $B_{_T}$ is symmetric in $m_1 \leftrightarrow m_2$.

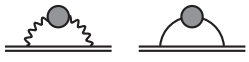
For understanding the UV asymptotics of the result, we need an expansion of the master integrals in inverse powers of $p_\perp^2$. Whereas A and $\dot{A}$ are independent of $p_\perp^2$, for B and $\dot{B}$ from eqs. (A.3) and (A.4) these limiting behaviours read

$$B(m_1,m_2) \approx B(0,0) + \frac{A(m_1)+A(m_2)}{p_\perp^2} + \mathcal{O}\Big(\frac{1}{p_\perp^4}\Big)\,, \quad B(0,0) \stackrel{d=3}{=} \frac{1}{8p_\perp}\,, \tag{A.7}$$

$$\dot{B}(m_1,m_2) \approx \frac{\dot{A}(m_1)+\dot{A}(m_2)}{p_\perp^2} + \mathcal{O}\Big(\frac{1}{p_\perp^4}\Big)\,. \tag{A.8}$$

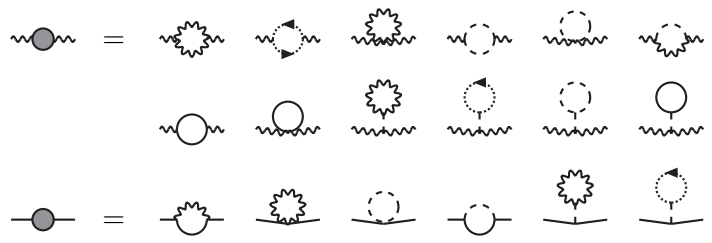
A.2. Z^0 self-energy

The Z^0 self-energy diagrams can be depicted as



, (A.9)

where the self-energies are



(A.10)

(A.11)

Here a wiggly line represents a spatial gauge field, a dotted line a ghost, a dashed line a Higgs field, and a solid line a temporal gauge field. The result reads

$$\begin{aligned}\Sigma(0) \quad \supset \quad & \frac{\tilde{g}^4 T^2}{4}\frac{i}{2}\int_{\mathbf{p}_\perp}\Bigg\{\frac{\Pi_T^Z}{(p_\perp^2+m_Z^2)^2} \\ & -\frac{\cos^2(\theta-\tilde{\theta})\,\Pi^{\tilde{Z}}}{(p_\perp^2+m_{\tilde{Z}}^2)^2}-\frac{\sin^2(\theta-\tilde{\theta})\,\Pi^{\tilde{Q}}}{(p_\perp^2+m_{\tilde{Q}}^2)^2}-\frac{\sin[2(\theta-\tilde{\theta})]\,\Pi^{\tilde{Z}\tilde{Q}}}{2(p_\perp^2+m_{\tilde{Z}}^2)(p_\perp^2+m_{\tilde{Q}}^2)}\Bigg\}. \end{aligned} \tag{A.12}$$

The transverse spatial self-energy reads

$$\begin{aligned}\Pi_T^Z \;=\;& A(m_{_H})\left[\frac{1}{2}\right] \\ +\;& A(m_{_Z})\left[\frac{(d-1)m_Z^2}{2m_H^2}\right] \\ +\;& A(m_{_W})\left[2(2-d)\cos^4(\theta)-\frac{2(p_\perp^2+m_W^2)\cos^2(\theta)}{m_Z^2}+\frac{(d-1)m_W^2}{m_H^2}\right] \\ +\;& A(m'_{_W})\left[2\cos^2(\theta)\,\frac{p_\perp^2+m_Z^2}{m_Z^2}\right] \\ +\;& A(m_{\widetilde{W}})\left[-2\cos^4(\theta)+\frac{m_W^2}{m_H^2}\right] \\ +\;& A(m_{\tilde{Z}})\left[\frac{m_Z^2\cos^2(\theta-\tilde{\theta})}{2m_H^2}\right] \\ +\;& A(m_{\tilde{Q}})\left[\frac{m_Z^2\sin^2(\theta-\tilde{\theta})}{2m_H^2}\right] \\ +\;& B(m_{_H},m_{_Z})\left[m_Z^2\right] \\ +\;& B(m_{_W},m_{_W})\left[\frac{2p_\perp^2(p_\perp^2+4m_W^2)\cos^2(\theta)}{m_Z^2}\right] \\ +\;& B(m_{_W},m'_{_W})\left[-\frac{2(p_\perp^2+m_Z^2)(p_\perp^2+2m_W^2-m_Z^2)\cos^2(\theta)}{m_Z^2}\right] \\ +\;& B_{_T}(m_{_H},m_{_Z})\left[1\right] \\ +\;& B_{_T}(m_{_W},m_{_W})\left[4(d-2)\cos^4(\theta)+\frac{(p_\perp^2+2m_W^2)^2}{m_Z^4}\right]\end{aligned}$$

$$
\begin{aligned}
&+ \quad B_{T}(m_{W}, m'_{W}) \left[-\frac{2(p_{\perp}^2 + m_{Z}^2)(p_{\perp}^2 + 2m_{W}^2 - m_{Z}^2)}{m_{Z}^4} \right] \\
&+ \quad B_{T}(m'_{W}, m'_{W}) \left[\frac{p_{\perp}^4 - m_{Z}^4}{m_{Z}^4} \right] \\
&+ \quad B_{T}(m_{\widetilde{W}}, m_{\widetilde{W}}) \left[4\cos^4(\theta) \right], \qquad \text{(A.13)}
\end{aligned}
$$

whereas the temporal parts can be expressed as

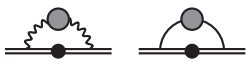
$$
\begin{aligned}
\Pi^{\tilde{Z}} &= A(m_{H}) \left[\frac{\cos^2(\theta - \tilde{\theta})}{2} \right] \\
&+ A(m_{Z}) \left[\frac{(d-1) m_{Z}^2 \cos^2(\theta - \tilde{\theta})}{2m_{H}^2} \right] \\
&+ A(m_{W}) \left[2(2-d)\cos^2(\theta)\cos^2(\tilde{\theta}) - \frac{2(p_{\perp}^2 + m_{\widetilde{W}}^2)\cos^2(\tilde{\theta})}{m_{Z}^2} + \frac{(d-1) m_{W}^2 \cos^2(\theta - \tilde{\theta})}{m_{H}^2} \right] \\
&+ A(m'_{W}) \left[\frac{2(p_{\perp}^2 + m_{\tilde{Z}}^2)\cos^2(\tilde{\theta})}{m_{Z}^2} \right] \\
&+ A(m_{\widetilde{W}}) \left[-2\cos^2(\theta)\cos^2(\tilde{\theta}) + \frac{m_{W}^2 \cos^2(\theta - \tilde{\theta})}{m_{H}^2} \right] \\
&+ A(m_{\tilde{Z}}) \left[\frac{m_{Z}^2 \cos^4(\theta - \tilde{\theta})}{2m_{H}^2} \right] \\
&+ A(m_{\widetilde{Q}}) \left[\frac{m_{Z}^2 \cos^2(\theta - \tilde{\theta}) \sin^2(\theta - \tilde{\theta})}{2m_{H}^2} \right] \\
&+ B(m_{H}, m_{\tilde{Z}}) \left[m_{Z}^2 \cos^4(\theta - \tilde{\theta}) \right] \\
&+ B(m_{H}, m_{\widetilde{Q}}) \left[m_{Z}^2 \cos^2(\theta - \tilde{\theta}) \sin^2(\theta - \tilde{\theta}) \right] \\
&+ B(m_{\widetilde{W}}, m_{W}) \left[\frac{2(p_{\perp}^4 + 2p_{\perp}^2 (m_{W}^2 + m_{\widetilde{W}}^2) + (m_{W}^2 - m_{\widetilde{W}}^2)^2)\cos^2(\tilde{\theta})}{m_{Z}^2} \right] \\
&+ B(m_{\widetilde{W}}, m'_{W}) \left[-\frac{2(p_{\perp}^2 + m_{\tilde{Z}}^2)(p_{\perp}^2 + 2m_{\widetilde{W}}^2 - m_{\tilde{Z}}^2)\cos^2(\tilde{\theta})}{m_{Z}^2} \right], \qquad \text{(A.14)} \\
\Pi^{\tilde{Z}\widetilde{Q}} &= A(m_{H}) \left[\frac{\sin(2(\theta - \tilde{\theta}))}{2} \right] \\
&+ A(m_{Z}) \left[\frac{(d-1) m_{Z}^2 \sin(2(\theta - \tilde{\theta}))}{2m_{H}^2} \right] \\
&+ A(m_{W}) \left[2(d-2)\cos^2(\theta)\sin(2\tilde{\theta}) + \frac{2(p_{\perp}^2 + m_{\widetilde{W}}^2)\sin(2\tilde{\theta})}{m_{Z}^2} + \frac{(d-1) m_{W}^2 \sin(2(\theta - \tilde{\theta}))}{m_{H}^2} \right] \\
&+ A(m'_{W}) \left[-\frac{(2p_{\perp}^2 + m_{\tilde{Z}}^2 + m_{\widetilde{Q}}^2)\sin(2\tilde{\theta})}{m_{Z}^2} \right] \\
&+ A(m_{\widetilde{W}}) \left[2\cos^2(\theta)\sin(2\tilde{\theta}) + \frac{m_{W}^2 \sin(2(\theta - \tilde{\theta}))}{m_{H}^2} \right]
\end{aligned}
$$

$$
\begin{aligned}
&+ \; A(m_{\tilde{Z}}) \left[\frac{m_Z^2 \cos^2(\theta-\tilde{\theta}) \sin(2(\theta-\tilde{\theta}))}{2m_H^2} \right] \\
&+ \; A(m_{\tilde{Q}}) \left[\frac{m_Z^2 \sin^2(\theta-\tilde{\theta}) \sin(2(\theta-\tilde{\theta}))}{2m_H^2} \right] \\
&+ \; B(m_H, m_{\tilde{Z}}) \left[m_Z^2 \cos^2(\theta-\tilde{\theta}) \sin(2(\theta-\tilde{\theta})) \right] \\
&+ \; B(m_H, m_{\tilde{Q}}) \left[m_Z^2 \sin^2(\theta-\tilde{\theta}) \sin(2(\theta-\tilde{\theta})) \right] \\
&+ \; B(m_{\widetilde{W}}, m_W) \left[-\frac{2(p_\perp^4 + 2p_\perp^2 (m_W^2 + m_{\widetilde{W}}^2) + (m_W^2 - m_{\widetilde{W}}^2)^2) \sin(2\tilde{\theta})}{m_Z^2} \right] \\
&+ \; B(m_{\widetilde{W}}, m'_W) \left[\frac{2(p_\perp^4 + 2p_\perp^2 m_{\widetilde{W}}^2 + m_{\widetilde{W}}^2 (m_{\tilde{Z}}^2 + m_{\tilde{Q}}^2) - m_{\tilde{Q}}^2 m_{\tilde{Z}}^2) \sin(2\tilde{\theta})}{m_Z^2} \right], \qquad \text{(A.15)}
\end{aligned}
$$

$$
\begin{aligned}
\Pi^{\tilde{Q}} \;=\; & A(m_H) \left[\frac{\sin^2(\theta-\tilde{\theta})}{2} \right] \\
&+ \; A(m_Z) \left[\frac{(d-1) m_Z^2 \sin^2(\theta-\tilde{\theta})}{2m_H^2} \right] \\
&+ \; A(m_W) \left[2(2-d) \cos^2(\theta) \sin^2(\tilde{\theta}) - \frac{2(p_\perp^2 + m_{\widetilde{W}}^2) \sin^2(\tilde{\theta})}{m_Z^2} + \frac{(d-1) m_W^2 \sin^2(\theta-\tilde{\theta})}{m_H^2} \right] \\
&+ \; A(m'_W) \left[\frac{2(p_\perp^2 + m_{\tilde{Q}}^2) \sin^2(\tilde{\theta})}{m_Z^2} \right] \\
&+ \; A(m_{\widetilde{W}}) \left[-2 \cos^2(\theta) \sin^2(\tilde{\theta}) + \frac{m_W^2 \sin^2(\theta-\tilde{\theta})}{m_H^2} \right] \\
&+ \; A(m_{\tilde{Z}}) \left[\frac{m_Z^2 \cos^2(\theta-\tilde{\theta}) \sin^2(\theta-\tilde{\theta})}{2m_H^2} \right] \\
&+ \; A(m_{\tilde{Q}}) \left[\frac{m_Z^2 \sin^4(\theta-\tilde{\theta})}{2m_H^2} \right] \\
&+ \; B(m_H, m_{\tilde{Z}}) \left[m_Z^2 \cos^2(\theta-\tilde{\theta}) \sin^2(\theta-\tilde{\theta}) \right] \\
&+ \; B(m_H, m_{\tilde{Q}}) \left[m_Z^2 \sin^4(\theta-\tilde{\theta}) \right] \\
&+ \; B(m_{\widetilde{W}}, m_W) \left[\frac{2(p_\perp^4 + 2p_\perp^2 (m_W^2 + m_{\widetilde{W}}^2) + (m_W^2 - m_{\widetilde{W}}^2)^2) \sin^2(\tilde{\theta})}{m_Z^2} \right] \\
&+ \; B(m_{\widetilde{W}}, m'_W) \left[-\frac{2(p_\perp^2 + m_{\tilde{Q}}^2)(p_\perp^2 + 2m_{\widetilde{W}}^2 - m_{\tilde{Q}}^2) \sin^2(\tilde{\theta})}{m_Z^2} \right]. \qquad \text{(A.16)}
\end{aligned}
$$

A.3. $W^\pm$ self-energy

The contribution of the $W^\pm$ self-energy diagrams, *viz.*



,

(A.17)

can be written as

$$\Sigma(0) \supset \frac{\tilde{g}^4 T^2 \cos^4(\theta)}{2} \frac{i}{2} \int_{\mathbf{p}_\perp} \left\{ \frac{\Pi_T^W}{(p_\perp^2 + m_W^2)^2} - \frac{\Pi^{\widetilde{W}}}{(p_\perp^2 + m_{\widetilde{W}}^2)^2} \right\}. \tag{A.18}$$

The transverse spatial self-energy reads

$$\begin{aligned}
\Pi_T^W &= A(m_H)\left[\frac{1}{2}\right] \\
&+ A(m_Z)\left[\left(2 - d - \frac{p_\perp^2 + m_W^2}{m_Z^2}\right)\cos^2(\theta) + \frac{(d-1)m_Z^2}{2m_H^2}\right] \\
&+ A(m'_Z)\left[\frac{(p_\perp^2 + m_W^2)\cos^2(\theta)}{m_Z^2}\right] \\
&+ A(m_W)\left[2 - d - \frac{p_\perp^2 + m_W^2}{m_W^2} + \frac{(d-1)m_W^2}{m_H^2}\right] \\
&+ A(m'_W)\left[\frac{p_\perp^2 + m_W^2}{m_W^2}\right] \\
&+ A(m_{\widetilde{W}})\left[-1 + \frac{m_W^2}{m_H^2}\right] \\
&+ A(m_{\tilde{Z}})\left[-\cos^2(\tilde{\theta}) + \frac{m_Z^2\cos^2(\theta - \tilde{\theta})}{2m_H^2}\right] \\
&+ A(m_{\tilde{Q}})\left[-\sin^2(\tilde{\theta}) + \frac{m_Z^2\sin^2(\theta - \tilde{\theta})}{2m_H^2}\right] \\
&+ B(m_H, m_W)\left[m_W^2\right] \\
&+ B(m_Z, m_W)\left[(m_W^2 + m_Z^2)\frac{p_\perp^4 + 2p_\perp^2(m_W^2 + m_Z^2) + (m_W^2 - m_Z^2)^2}{m_Z^4}\right] \\
&+ B(m_Z, m'_W)\left[-\frac{(p_\perp^2 + m_W^2)(p_\perp^2 + 2m_Z^2 - m_W^2)}{m_Z^2}\right] \\
&+ B(m'_Z, m_W)\left[-\frac{(p_\perp^2 + m_W^2)^2\cos^2(\theta)}{m_Z^2}\right] \\
&+ B(0, m_W)\left[\frac{(p_\perp^4 + 4p_\perp^2 m_W^2 - m_W^4)\sin^2(\theta)}{m_W^2}\right] \\
&+ B(0, m'_W)\left[\frac{(m_W^4 - p_\perp^4)\sin^2(\theta)}{m_W^2}\right] \\
&+ \left[\frac{B(m_W, m_Q) - B(m_W, m'_Q)}{m_Q^2} + \frac{A(m'_Q) - A(m_Q)}{m_Q^2(p_\perp^2 + m_W^2)}\right]\left[(p_\perp^2 + m_W^2)^2\sin^2(\theta)\right] \\
&+ B_T(m_H, m_W)\left[1\right] \\
&+ B_T(m_Z, m_W)\left[4(d-2)\cos^2(\theta) + \frac{p_\perp^4 + 2p_\perp^2(m_W^2 + m_Z^2) + (m_W^2 + m_Z^2)^2}{m_Z^4}\right]
\end{aligned}$$

$$
\begin{aligned}
&+ \quad B_{T}(m_{Z},m'_{W})\left[-\frac{(p_{\perp}^{2}+m_{W}^{2})(p_{\perp}^{2}+2m_{Z}^{2}-m_{W}^{2})}{m_{Z}^{4}}\right]\\
&+ \quad B_{T}(m'_{Z},m_{W})\left[-\frac{(p_{\perp}^{2}+m_{W}^{2})^{2}}{m_{Z}^{4}}\right]\\
&+ \quad B_{T}(m'_{W},m'_{Z})\left[\frac{p_{\perp}^{4}-m_{W}^{4}}{m_{Z}^{4}}\right]\\
&+ \quad B_{T}(0,m_{W})\left[4(d-2)\sin^{2}(\theta)+\frac{2(p_{\perp}^{2}+m_{W}^{2})\sin^{2}(\theta)}{m_{W}^{2}}\right]\\
&+ \quad B_{T}(0,m'_{W})\left[-\frac{2(p_{\perp}^{2}+m_{W}^{2})\sin^{2}(\theta)}{m_{W}^{2}}\right]\\
&+ \quad B_{T}(m_{\tilde{Z}},m_{\widetilde{W}})\left[4\cos^{2}(\tilde{\theta})\right]\\
&+ \quad B_{T}(m_{\tilde{Q}},m_{\widetilde{W}})\left[4\sin^{2}(\tilde{\theta})\right]\\
&+ \quad \frac{B_{T}(m'_{W},m_{Q})-B_{T}(m'_{W},m'_{Q})}{m_{Q}^{2}}\left[\frac{(m_{W}^{4}-p_{\perp}^{4})\sin^{2}(\theta)}{m_{W}^{2}}\right]\\
&+ \quad \frac{B_{T}(m_{W},m_{Q})-B_{T}(m_{W},m'_{Q})}{m_{Q}^{2}}\left[\frac{(p_{\perp}^{2}+m_{W}^{2})^{2}\sin^{2}(\theta)}{m_{W}^{2}}\right], \qquad \text{(A.19)}
\end{aligned}
$$

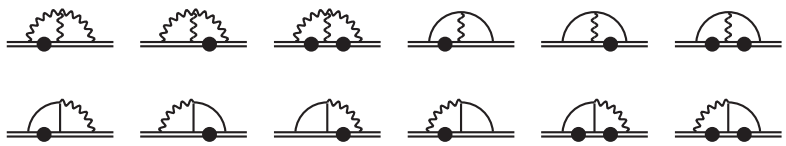
whereas the temporal part can be expressed as

$$
\begin{aligned}
\Pi^{\widetilde{W}} \quad = \quad & A(m_{H})\left[\frac{1}{2}\right]\\
&+ \quad A(m_{Z})\left[\left(2-d-\frac{p_{\perp}^{2}+m_{\widetilde{W}}^{2}}{m_{Z}^{2}}\right)\cos^{2}(\theta)+\frac{(d-1)m_{Z}^{2}}{2m_{H}^{2}}\right]\\
&+ \quad A(m'_{Z})\left[\frac{(p_{\perp}^{2}+m_{\widetilde{W}}^{2})\cos^{2}(\theta)}{m_{Z}^{2}}\right]\\
&+ \quad A(m_{W})\left[2-d-\frac{(p_{\perp}^{2}+m_{\tilde{Z}}^{2})\cos^{2}(\tilde{\theta})}{m_{W}^{2}}-\frac{(p_{\perp}^{2}+m_{\tilde{Q}}^{2})\sin^{2}(\tilde{\theta})}{m_{W}^{2}}+\frac{(d-1)m_{W}^{2}}{m_{H}^{2}}\right]\\
&+ \quad A(m'_{W})\left[\frac{p_{\perp}^{2}+m_{\widetilde{W}}^{2}}{m_{W}^{2}}\right]\\
&+ \quad A(m_{\widetilde{W}})\left[-1+\frac{m_{W}^{2}}{m_{H}^{2}}\right]\\
&+ \quad A(m_{\tilde{Z}})\left[-\cos^{2}(\tilde{\theta})+\frac{m_{Z}^{2}\cos^{2}(\theta-\tilde{\theta})}{2m_{H}^{2}}\right]\\
&+ \quad A(m_{\tilde{Q}})\left[-\sin^{2}(\tilde{\theta})+\frac{m_{Z}^{2}\sin^{2}(\theta-\tilde{\theta})}{2m_{H}^{2}}\right]\\
&+ \quad B(m_{H},m_{\widetilde{W}})\left[m_{W}^{2}\right]\\
&+ \quad B(m_{Z},m_{\widetilde{W}})\left[\frac{(p_{\perp}^{4}+2p_{\perp}^{2}(m_{\widetilde{W}}^{2}+m_{Z}^{2})+(m_{\widetilde{W}}^{2}-m_{Z}^{2})^{2})\cos^{2}(\theta)}{m_{Z}^{2}}\right]
\end{aligned}
$$

$$
\begin{aligned}
&+ \quad B(m'_Z, m_{\widetilde{W}}) \left[-\frac{(p_\perp^2 + m_{\widetilde{W}}^2)^2 \cos^2(\theta)}{m_Z^2} \right] \\
&+ \quad B(m_{\tilde{Z}}, m_W) \left[\frac{(p_\perp^4 + 2p_\perp^2 (m_W^2 + m_{\tilde{Z}}^2) + (m_W^2 - m_{\tilde{Z}}^2)^2) \cos^2(\tilde{\theta})}{m_W^2} \right] \\
&+ \quad B(m_{\tilde{Q}}, m_W) \left[\frac{(p_\perp^4 + 2p_\perp^2 (m_W^2 + m_{\tilde{Q}}^2) + (m_W^2 - m_{\tilde{Q}}^2)^2) \sin^2(\tilde{\theta})}{m_W^2} \right] \\
&+ \quad B(m_{\tilde{Z}}, m'_W) \left[-\frac{(p_\perp^2 + m_{\widetilde{W}}^2)(p_\perp^2 + 2m_{\tilde{Z}}^2 - m_{\widetilde{W}}^2) \cos^2(\tilde{\theta})}{m_W^2} \right] \\
&+ \quad B(m_{\tilde{Q}}, m'_W) \left[-\frac{(p_\perp^2 + m_{\widetilde{W}}^2)(p_\perp^2 + 2m_{\tilde{Q}}^2 - m_{\widetilde{W}}^2) \sin^2(\tilde{\theta})}{m_W^2} \right] \\
&+ \quad \left[\frac{B(m_{\widetilde{W}}, m_Q) - B(m_{\widetilde{W}}, m'_Q)}{m_Q^2} + \frac{A(m'_Q) - A(m_Q)}{m_Q^2 (p_\perp^2 + m_{\widetilde{W}}^2)} \right] \left[(p_\perp^2 + m_{\widetilde{W}}^2)^2 \sin^2(\theta) \right] \\
&+ \quad B(0, m_{\widetilde{W}}) \left[2(p_\perp^2 - m_{\widetilde{W}}^2) \sin^2(\theta) \right] . \qquad \text{(A.20)}
\end{aligned}
$$

A.4. Triple gauge vertex

The contribution of triple gauge vertex diagrams, *viz.*



, (A.21)

can be written as

$$
\begin{aligned}
\Sigma(0) \quad \supset \quad & \frac{\tilde{g}^4 T^2 \cos^3(\theta)}{2} \frac{i}{2} \int_{\mathbf{p}_\perp} \left\{ \frac{\Upsilon^Z}{p_\perp^2 + m_Z^2} + \frac{\Upsilon^W}{p_\perp^2 + m_W^2} \right. \\
& \left. - \frac{\Upsilon^{\tilde{Z}}}{p_\perp^2 + m_{\tilde{Z}}^2} - \frac{\Upsilon^{\tilde{Q}}}{p_\perp^2 + m_{\tilde{Q}}^2} - \frac{\Upsilon^{\widetilde{W}}}{p_\perp^2 + m_{\widetilde{W}}^2} \right\} , \qquad \text{(A.22)}
\end{aligned}
$$

where

$$
\begin{aligned}
\Upsilon^Z &= \cos(\theta) \left[\theta_{zz}(m_W, m_W) + 2B(m_{\widetilde{W}}, m_{\widetilde{W}}) \right] , \qquad \text{(A.23)} \\
\Upsilon^W &= 2\cos(\theta) \left[\cos^2(\theta) \theta_{zz}(m_Z, m_W) + 2\cos^2(\tilde{\theta}) B(m_{\tilde{Z}}, m_{\widetilde{W}}) \right] \\
&+ 2\cos(\theta) \left[\sin^2(\theta) \theta_{zz}(m_Q, m_W) + 2\sin^2(\tilde{\theta}) B(m_{\tilde{Q}}, m_{\widetilde{W}}) \right] , \qquad \text{(A.24)} \\
\Upsilon^{\tilde{Z}} &= 2\cos(\tilde{\theta}) \cos(\theta - \tilde{\theta}) \, \theta_{z0}(m_W, m_{\widetilde{W}}) , \qquad \text{(A.25)} \\
\Upsilon^{\tilde{Q}} &= -2\sin(\tilde{\theta}) \sin(\theta - \tilde{\theta}) \, \theta_{z0}(m_W, m_{\widetilde{W}}) , \qquad \text{(A.26)} \\
\Upsilon^{\widetilde{W}} &= 2\cos(\theta) \left[\cos^2(\theta) \theta_{z0}(m_Z, m_{\widetilde{W}}) + \cos^2(\tilde{\theta}) \theta_{z0}(m_W, m_{\tilde{Z}}) \right] \\
&+ 2\cos(\theta) \left[\sin^2(\theta) \theta_{z0}(m_Q, m_{\widetilde{W}}) + \sin^2(\tilde{\theta}) \theta_{z0}(m_W, m_{\tilde{Q}}) \right] . \qquad \text{(A.27)}
\end{aligned}
$$

Here we have denoted

$$\theta_{zz}(m_1,m_2) \equiv \int_{\mathbf{q}} \mathbb{P}\left\{\frac{\gamma_{3ij}(p,q)}{q_z}\,\Delta_{3i}(q,m_1)\Delta_{3j}(p+q,m_2)\right\}_{p_z=0} \tag{A.28}$$

$$= \frac{A(m_1)-A(m_1')}{m_1^2}+\frac{A(m_2)-A(m_2')}{m_2^2}+\frac{p_\perp^2[B_T(m_1,m_2)-B_T(m_1',m_2')]}{m_1^2m_2^2}$$
$$+ \frac{p_\perp^2+m_1^2}{m_2^2}\left[B(m_1,m_2')-B(m_1,m_2)+\frac{B_T(m_1,m_2')-B_T(m_1,m_2)}{m_1^2}\right]$$
$$+ \frac{p_\perp^2+m_2^2}{m_1^2}\left[B(m_1',m_2)-B(m_1,m_2)+\frac{B_T(m_1',m_2)-B_T(m_1,m_2)}{m_2^2}\right], \tag{A.29}$$

$$\theta_{z0}(m_1,m_2) \equiv \int_{\mathbf{q}} \mathbb{P}\left\{\frac{\tilde\gamma_{3ij}(p,q)}{q_z}\,\Delta_{ij}(q,m_1)\Delta_{00}(p+q,m_2)\right\}_{p_z=0} \tag{A.30}$$

$$= B(m_1,m_2)+\frac{A(m_1)-A(m_1')}{m_1^2}$$
$$+ \frac{p_\perp^2+m_2^2}{m_1^2}\left[B(m_1',m_2)-B(m_1,m_2)\right], \tag{A.31}$$

where

$$\gamma_{3ij}(p,q) \equiv \delta_{3i}(q_j-p_j)+\delta_{3j}(q_i+2p_i)-\delta_{ij}(2q_z+p_z)\,, \tag{A.32}$$

$$\tilde\gamma_{3ij}(p,q) \equiv \delta_{3j}(q_i+2p_i)\,, \tag{A.33}$$

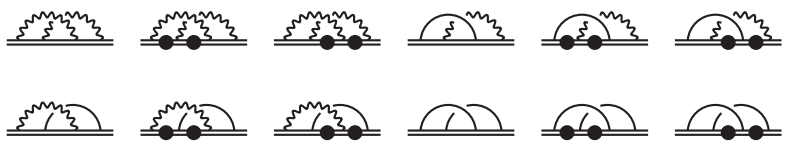
$$\Delta_{00}(p,m) \equiv \frac{1}{p^2+m^2}\,, \tag{A.34}$$

$$\Delta_{ij}(p,m) \equiv \frac{\delta_{ij}}{p^2+m^2}+\frac{p_ip_j}{m^2}\left(\frac{1}{p^2+m^2}-\frac{1}{p^2+m'^2}\right). \tag{A.35}$$

We note that θ_{zz} is symmetric in $m_1 \leftrightarrow m_2$.

A.5. Crossed fermion self-energy

For the "crossed" NLO self-energy diagrams, *viz.*



(A.36)

the result can be written as

$$\begin{aligned}
\Sigma(0) \;\supset\; & \frac{\tilde{g}^4T^2}{16}\Big\{\phi_{zz}(m_{\scriptscriptstyle Z},m_{\scriptscriptstyle Z}) \\
& -2\cos^2(\theta-\tilde{\theta})\phi_{0z}(m_{\tilde{Z}},m_{\scriptscriptstyle Z}) - 2\sin^2(\theta-\tilde{\theta})\phi_{0z}(m_{\tilde{Q}},m_{\scriptscriptstyle Z}) \\
& +\cos^4(\theta-\tilde{\theta})\phi_{00}(m_{\tilde{Z}},m_{\tilde{Z}}) + \sin^4(\theta-\tilde{\theta})\phi_{00}(m_{\tilde{Q}},m_{\tilde{Q}}) \\
& +2\cos^2(\theta-\tilde{\theta})\sin^2(\theta-\tilde{\theta})\phi_{00}(m_{\tilde{Z}},m_{\tilde{Q}}) \\
+\;\; & 4\cos^2(\theta)\Big[\cos(2\theta)\Big(\phi_{z0}(m_{\scriptscriptstyle Z},m_{\widetilde{W}}) - \phi_{zz}(m_{\scriptscriptstyle Z},m_{\scriptscriptstyle W})\Big) \\
& +\cos(\theta-\tilde{\theta})\cos(\theta+\tilde{\theta})\Big(\phi_{0z}(m_{\tilde{Z}},m_{\scriptscriptstyle W}) - \phi_{00}(m_{\tilde{Z}},m_{\widetilde{W}})\Big) \\
& +\sin(\theta-\tilde{\theta})\sin(\theta+\tilde{\theta})\Big(\phi_{00}(m_{\tilde{Q}},m_{\widetilde{W}}) - \phi_{0z}(m_{\tilde{Q}},m_{\scriptscriptstyle W})\Big)\Big]\Big\}\,, \qquad \text{(A.37)}
\end{aligned}$$

where

$$\phi_{ij}(m_1,m_2) \;\equiv\; \int_{\mathbf{p},\mathbf{q}} \frac{\Delta_{ii}(p,m_1)\Delta_{jj}(q,m_2)}{(p_z-i0^+)(p_z+q_z-i0^+)(q_z-i0^+)}\,, \qquad \text{(A.38)}$$

and the propagators are from eqs. (A.34) and (A.35). The integrals over p_z, q_z can be carried out by contour integration, most simply by closing in the lower half-plane so that the denominators in eq. (A.38) have no pole, or alternatively by inserting eq. (3.2). For the part $\propto p_z^2$ from eq. (A.35), this yields contributions which are directly identified with the master functions A, B from sec. A.1. The other parts require some more work, either by writing $1/p_z^2 = \partial_{p_z}(-1/p_z)$ and carrying out a partial integration, or by resorting to contour integration. In this way we obtain ($\epsilon_{pi} \equiv \sqrt{p_\perp^2+m_i^2}$)

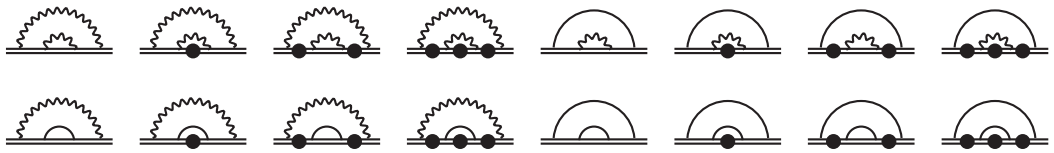
$$\phi_{00}(m_1,m_2) \;=\; -\frac{i}{4}\int_{\mathbf{p}_\perp,\mathbf{q}_\perp} \frac{1}{\epsilon_{p1}^2\epsilon_{q2}^2(\epsilon_{p1}+\epsilon_{q2})} = i\int_{\mathbf{p}_\perp}\left\{\frac{\dot{A}(m_2)}{p_\perp^2+m_1^2} + \frac{\dot{A}(m_1)}{p_\perp^2+m_2^2} - \dot{B}(m_1,m_2)\right\}, \qquad \text{(A.39)}$$

where in the last step we substituted integration variables and re-expressed the result in terms of the master integrals from sec. A.1, evaluated with $p_z = 0$. The other integrals read

$$\begin{aligned}
\phi_{0z}(m_1,m_2) &= \phi_{z0}(m_2,m_1) \\
&= \phi_{00}(m_1,m_2) \\
&+ \frac{i}{2}\int_{\mathbf{p}_\perp}\left\{\frac{1}{m_2^2}\left[\frac{A(m_2)-A(m_2')}{p_\perp^2+m_1^2} + B(m_1,m_2') - B(m_1,m_2)\right]\right\}, \qquad \text{(A.40)} \\
\phi_{zz}(m_1,m_2) &= \phi_{0z}(m_1,m_2) \\
&+ \frac{i}{2}\int_{\mathbf{p}_\perp}\left\{\frac{1}{m_1^2}\left[\frac{A(m_1)-A(m_1')}{p_\perp^2+m_2^2} + B(m_1',m_2) - B(m_1,m_2)\right]\right. \\
&- \left.\frac{B_{\scriptscriptstyle T}(m_1,m_2) - B_{\scriptscriptstyle T}(m_1',m_2) - B_{\scriptscriptstyle T}(m_1,m_2') + B_{\scriptscriptstyle T}(m_1',m_2')}{m_1^2m_2^2}\right\}. \qquad \text{(A.41)}
\end{aligned}$$

A.6. Uncrossed fermion self-energy

The result for the "uncrossed" NLO self-energy diagrams, *viz.*



can be written as

$$
\begin{aligned}
\Sigma(0) \;\supset\; & \frac{\tilde{g}^4T^2}{16}\Big\{\chi_{zz}(m_Z,m_Z) - \cos^2(\theta-\tilde{\theta})\chi_{0z}(m_{\widetilde{Z}},m_Z) - \sin^2(\theta-\tilde{\theta})\chi_{0z}(m_{\widetilde{Q}},m_Z) \\
& \quad - \cos^2(\theta-\tilde{\theta})\chi_{z0}(m_Z,m_{\widetilde{Z}}) - \sin^2(\theta-\tilde{\theta})\chi_{z0}(m_Z,m_{\widetilde{Q}}) \\
& \quad + \cos^4(\theta-\tilde{\theta})\chi_{00}(m_{\widetilde{Z}},m_{\widetilde{Z}}) + \sin^4(\theta-\tilde{\theta})\chi_{00}(m_{\widetilde{Q}},m_{\widetilde{Q}}) \\
& \quad + \cos^2(\theta-\tilde{\theta})\sin^2(\theta-\tilde{\theta})\Big[\chi_{00}(m_{\widetilde{Z}},m_{\widetilde{Q}}) + \chi_{00}(m_{\widetilde{Q}},m_{\widetilde{Z}})\Big] \\
+ \;& 2\cos^2(\theta)\Big[\chi_{zz}(m_Z,m_W) - \cos^2(\theta-\tilde{\theta})\chi_{0z}(m_{\widetilde{Z}},m_W) - \sin^2(\theta-\tilde{\theta})\chi_{0z}(m_{\widetilde{Q}},m_W) \\
& \quad - \chi_{z0}(m_Z,m_{\widetilde{W}}) + \cos^2(\theta-\tilde{\theta})\chi_{00}(m_{\widetilde{Z}},m_{\widetilde{W}}) + \sin^2(\theta-\tilde{\theta})\chi_{00}(m_{\widetilde{Q}},m_{\widetilde{W}})\Big] \\
+ \;& 4\cos^4(\theta)\Big[\chi_{zz}(m_W,m_W) - \chi_{0z}(m_{\widetilde{W}},m_W) - \chi_{z0}(m_W,m_{\widetilde{W}}) + \chi_{00}(m_{\widetilde{W}},m_{\widetilde{W}})\Big] \\
+ \;& 2\cos^2(\theta)\Big[\cos^2(2\theta)\,\chi_{zz}(m_W,m_Z) - \cos^2(2\theta)\,\chi_{0z}(m_{\widetilde{W}},m_Z) \\
& \quad - \cos^2(\theta+\tilde{\theta})\chi_{z0}(m_W,m_{\widetilde{Z}}) + \cos^2(\theta+\tilde{\theta})\chi_{00}(m_{\widetilde{W}},m_{\widetilde{Z}})\Big] \\
+ \;& 2\cos^2(\theta)\Big[\sin^2(2\theta)\,\chi_{zz}(m_W,m_Q) - \sin^2(2\theta)\,\chi_{0z}(m_{\widetilde{W}},m_Q) \\
& \quad - \sin^2(\theta+\tilde{\theta})\chi_{z0}(m_W,m_{\widetilde{Q}}) + \sin^2(\theta+\tilde{\theta})\chi_{00}(m_{\widetilde{W}},m_{\widetilde{Q}})\Big]\Big\}\,,
\end{aligned}
\tag{A.42}
$$

where, making use of Δ_{ij} defined according to eqs. (A.34) and (A.35),

$$
\chi_{ij}(m_1,m_2) \;\equiv\; \int_{\mathbf{p},\mathbf{q}} \frac{\Delta_{ii}(p,m_1)\Delta_{jj}(q,m_2)}{(p_z-i0^+)^2(p_z+q_z-i0^+)}\,. \tag{A.43}
$$

For dealing with the double pole in eq. (A.43), it is convenient to write

$$
\begin{aligned}
\frac{1}{(p_z-i0^+)^2(p_z+q_z-i0^+)} \;=\; & -\frac{1}{(p_z-i0^+)(p_z+q_z-i0^+)(q_z-i0^+)} \\
& + \frac{1}{(p_z-i0^+)(p_z+q_z-i0^+)}\underbrace{\left(\frac{1}{p_z-i0^+}+\frac{1}{q_z-i0^+}\right)}_{\frac{p_z+q_z-i0^+}{(p_z-i0^+)(q_z-i0^+)}}\,.
\end{aligned}
\tag{A.44}
$$

Therefore

$$
\chi_{ij}(m_1,m_2) = -\phi_{ij}(m_1,m_2) + \delta\chi_{ij}(m_1,m_2)\,, \tag{A.45}
$$

where ϕ_{ij} is from eqs. (A.39)–(A.41) and

$$\delta\chi_{ij}(m_1,m_2) \;=\; \int_{\mathbf{p}} \frac{\Delta_{ii}(p,m_1)}{(p_z-i0^+)^2} \int_{\mathbf{q}} \frac{\Delta_{jj}(q,m_2)}{q_z-i0^+} \,. \tag{A.46}$$

These integrals can be carried out by contour integration, or by making use of eq. (3.2), noting that $\Delta(q,m_2)$ is odd in q_z so that only the imaginary part contributes, and removing $1/p_z^2$ from the other term through partial integration, like around eq. (A.39). This yields

$$\begin{aligned} \delta\chi_{00}(m_1,m_2) &= \delta\chi_{0z}(m_1,m_2) \,=\, \frac{i}{2}\int_{\mathbf{p}_\perp} \frac{1}{p_\perp^2+m_2^2} \big[\, 2\,\dot{A}(m_1)\,\big] \,, & \text{(A.47)} \\ \delta\chi_{z0}(m_1,m_2) &= \delta\chi_{zz}(m_1,m_2) \\ &= \delta\chi_{00}(m_1,m_2) \,+\, \frac{i}{2}\int_{\mathbf{p}_\perp} \frac{1}{p_\perp^2+m_2^2} \left[\, \frac{A(m_1)-A(m_1')}{m_1^2} \,\right] . & \text{(A.48)} \end{aligned}$$

The contributions from $\delta\chi$ are closely related to those in sec. A.7.

A.7. Wave function normalization

The final contribution originates from the second term in eq. (3.3), with the various channels of fig. 1 contributing with coefficients like in eq. (3.4). The tree-level part of the self-energy, k_z, gets corrected by this term (cf. eq. (2.5)), and the correction needs to be factored out, in order to determine the location of the pole of the corresponding propagator. In other words, we write the combination appearing in eq. (2.5) as

$$\begin{aligned} k_z + \Sigma(k_z) &= k_z\big[1+\Sigma'(0)\big] + \Sigma(0) + \mathcal{O}(k_z^2) \\ &= \big[1+\Sigma'(0)\big]\Big[k_z + \frac{\Sigma(0)}{1+\Sigma'(0)}\Big] + \mathcal{O}(k_z^2) \,. \end{aligned} \tag{A.49}$$

This implies that, up to NNLO corrections, the physical width is

$$\frac{\Gamma_u}{2} \approx \mathrm{Im}\left[\frac{\Sigma(0)}{1+\Sigma'(0)}\right] = \mathrm{Im}\,\Sigma_{\rm LO}(0) + \big\{\,\mathrm{Im}\,\Sigma_{\rm NLO}(0) - \Sigma'_{\rm LO}(0)\;\mathrm{Im}\,\Sigma_{\rm LO}(0)\,\big\} + \mathcal{O}\biggl(\frac{\tilde{g}^6T^3}{m_i^2}\biggr) \,. \tag{A.50}$$

The last term shown reads

$$\begin{aligned} -i\,\Sigma'_{\rm LO}(0)\;\mathrm{Im}\,\Sigma_{\rm LO}(0) &= -\frac{\tilde{g}^4T^2}{16}\frac{i}{2}\int_{\mathbf{p}_\perp} \biggl\{ \frac{1}{p_\perp^2+m_Z^2} - \frac{\cos^2(\theta-\tilde{\theta})}{p_\perp^2+m_{\tilde{Z}}^2} - \frac{\sin^2(\theta-\tilde{\theta})}{p_\perp^2+m_{\tilde{Q}}^2} \\ &\qquad + 2\cos^2(\theta)\biggl[\frac{1}{p_\perp^2+m_W^2} - \frac{1}{p_\perp^2+m_{\widetilde{W}}^2}\biggr]\biggr\} \\ &\quad\times\; \biggl\{ \frac{A(m_Z)-A(m_Z')}{m_Z^2} + 2\cos^2(\theta)\,\frac{A(m_W)-A(m_W')}{m_W^2} \\ &\qquad + 2\big[\dot{A}(m_Z) - \cos^2(\theta-\tilde{\theta})\dot{A}(m_{\tilde{Z}}) - \sin^2(\theta-\tilde{\theta})\dot{A}(m_{\tilde{Q}})\big] \\ &\qquad + 4\cos^2(\theta)\big[\dot{A}(m_W) - \dot{A}(m_{\widetilde{W}})\big]\biggr\} \,. \end{aligned} \tag{A.51}$$

References

[1] P. Minkowski, $\mu \to e\gamma$ *at a Rate of One Out of* 10^9 *Muon Decays?,* Phys. Lett. B 67 (1977) 421.

[2] M. Gell-Mann, P. Ramond and R. Slansky, *Complex Spinors and Unified Theories,* Conf. Proc. C 790927 (1979) 315 [1306.4669].

[3] T. Yanagida, *Horizontal Symmetry and Masses of Neutrinos,* Prog. Theor. Phys. 64 (1980) 1103.

[4] E.K. Akhmedov, V.A. Rubakov and A.Y. Smirnov, *Baryogenesis via neutrino oscillations,* Phys. Rev. Lett. 81 (1998) 1359 [hep-ph/9803255].

[5] T. Asaka and M. Shaposhnikov, *The νMSM, dark matter and baryon asymmetry of the universe,* Phys. Lett. B 620 (2005) 17 [hep-ph/0505013].

[6] M. Chrzaszcz, M. Drewes, T.E. Gonzalo, J. Harz, S. Krishnamurthy and C. Weniger, *A frequentist analysis of three right-handed neutrinos with GAMBIT,* 1908.02302.

[7] M. Drewes, B. Garbrecht, D. Gueter and J. Klarić, *Leptogenesis from Oscillations of Heavy Neutrinos with Large Mixing Angles,* JHEP 12 (2016) 150 [1606.06690].

[8] P. Hernández, M. Kekic, J. López-Pavón, J. Racker and J. Salvado, *Testable Baryogenesis in Seesaw Models,* JHEP 08 (2016) 157 [1606.06719].

[9] T. Hambye and D. Teresi, *Baryogenesis from L-violating Higgs-doublet decay in the density-matrix formalism,* Phys. Rev. D 96 (2017) 015031 [1705.00016].

[10] A. Abada, G. Arcadi, V. Domcke and M. Lucente, *Neutrino masses, leptogenesis and dark matter from small lepton number violation?,* JCAP 12 (2017) 024 [1709.00415].

[11] J. Ghiglieri and M. Laine, *GeV-scale hot sterile neutrino oscillations: a numerical solution,* JHEP 02 (2018) 078 [1711.08469].

[12] S. Eijima, M. Shaposhnikov and I. Timiryasov, *Parameter space of baryogenesis in the νMSM,* JHEP 07 (2019) 077 [1808.10833].

[13] M. Shaposhnikov, *The νMSM, leptonic asymmetries, and properties of singlet fermions,* JHEP 08 (2008) 008 [0804.4542].

[14] L. Canetti, M. Drewes, T. Frossard and M. Shaposhnikov, *Dark Matter, Baryogenesis and Neutrino Oscillations from Right Handed Neutrinos,* Phys. Rev. D 87 (2013) 093006 [1208.4607].

[15] S. Eijima and M. Shaposhnikov, *Fermion number violating effects in low scale leptogenesis,* Phys. Lett. B 771 (2017) 288 [1703.06085].

[16] J. Ghiglieri and M. Laine, *Sterile neutrino dark matter via GeV-scale leptogenesis?,* JHEP 07 (2019) 078 [1905.08814].

[17] X.-D. Shi and G.M. Fuller, *A New dark matter candidate: Nonthermal sterile neutrinos,* Phys. Rev. Lett. 82 (1999) 2832 [astro-ph/9810076].

[18] M. Laine and M. Shaposhnikov, *Sterile neutrino dark matter as a consequence of νMSM-induced lepton asymmetry,* JCAP 06 (2008) 031 [0804.4543].

[19] J. Ghiglieri and M. Laine, *Improved determination of sterile neutrino dark matter spectrum,* JHEP 11 (2015) 171 [1506.06752].

[20] M. Laine, *Thermal right-handed neutrino production rate in the relativistic regime,* JHEP 08 (2013) 138 [1307.4909].

[21] I. Ghisoiu and M. Laine, *Right-handed neutrino production rate at $T > 160$ GeV,* JCAP 12 (2014) 032 [1411.1765].

[22] S. Biondini, N. Brambilla and A. Vairo, *CP asymmetry in heavy Majorana neutrino decays at finite temperature: the hierarchical case,* JHEP 09 (2016) 126 [1608.01979].

[23] D. Bödeker and M. Sangel, *Lepton asymmetry rate from quantum field theory: NLO in the hierarchical limit,* JCAP 06 (2017) 052 [1702.02155].

[24] J. Racker, *Unitarity and CP violation in leptogenesis at NLO: general considerations and top Yukawa contributions,* JHEP 02 (2019) 042 [1811.00280].

[25] S. Caron-Huot, *$O(g)$ plasma effects in jet quenching,* Phys. Rev. D 79 (2009) 065039 [0811.1603].

[26] P. Aurenche, F. Gelis and H. Zaraket, *A Simple sum rule for the thermal gluon spectral function and applications,* JHEP 05 (2002) 043 [hep-ph/0204146].

[27] J. Ghiglieri, J. Hong, A. Kurkela, E. Lu, G.D. Moore and D. Teaney, *Next-to-leading order thermal photon production in a weakly coupled quark-gluon plasma,* JHEP 05 (2013) 010 [1302.5970].

[28] J. Ghiglieri and G.D. Moore, *Low Mass Thermal Dilepton Production at NLO in a Weakly Coupled Quark-Gluon Plasma,* JHEP 12 (2014) 029 [1410.4203].

[29] J. Ghiglieri, G.D. Moore and D. Teaney, *QCD Shear Viscosity at (almost) NLO,* JHEP 03 (2018) 179 [1802.09535].

[30] M. Laine, *A non-perturbative contribution to jet quenching,* Eur. Phys. J. C 72 (2012) 2233 [1208.5707].

[31] M. Laine and A. Rothkopf, *Light-cone Wilson loop in classical lattice gauge theory,* JHEP 07 (2013) 082 [1304.4443].

[32] M. Panero, K. Rummukainen and A. Schäfer, *Lattice Study of the Jet Quenching Parameter,* Phys. Rev. Lett. 112 (2014) 162001 [1307.5850].

[33] M. D'Onofrio, A. Kurkela and G.D. Moore, *Renormalization of Null Wilson Lines in EQCD,* JHEP 03 (2014) 125 [1401.7951].

[34] D. Bödeker and M. Laine, *Kubo relations and radiative corrections for lepton number washout,* JCAP 05 (2014) 041 [1403.2755].

[35] D. Bödeker and M. Sangel, *Order g^2 susceptibilities in the symmetric phase of the Standard Model,* JCAP 04 (2015) 040 [1501.03151].

[36] H.A. Weldon, *Effective fermion masses of order gT in high-temperature gauge theories with exact chiral invariance,* Phys. Rev. D 26 (1982) 2789.

[37] J. Ghiglieri and M. Laine, *Precision study of GeV-scale resonant leptogenesis,* JHEP 02 (2019) 014 [1811.01971].

[38] J. Ghiglieri and D. Teaney, *Parton energy loss and momentum broadening at NLO in high temperature QCD plasmas,* Int. J. Mod. Phys. E 24 (2015) 1530013 [1502.03730].

[39] J. Ghiglieri, G.D. Moore and D. Teaney, *Jet-Medium Interactions at NLO in a Weakly-Coupled Quark-Gluon Plasma,* JHEP 03 (2016) 095 [1509.07773].

[40] K. Kajantie, M. Laine, K. Rummukainen and M.E. Shaposhnikov, *Generic rules for high temperature dimensional reduction and their application to the Standard Model,* Nucl. Phys. B 458 (1996) 90 [hep-ph/9508379].

[41] J. Ghiglieri and M. Laine, *Neutrino dynamics below the electroweak crossover,* JCAP 07 (2016) 015 [1605.07720].

[42] M. D'Onofrio, K. Rummukainen and A. Tranberg, *Sphaleron Rate in the Minimal Standard Model,* Phys. Rev. Lett. 113 (2014) 141602 [1404.3565].